

See discussions, stats, and author profiles for this publication at: <https://www.researchgate.net/publication/256075261>

# Why the Partition Coefficient of Ionic Liquids Is Concentration-Dependent

ARTICLE in THE JOURNAL OF PHYSICAL CHEMISTRY B · AUGUST 2013

Impact Factor: 3.3 · DOI: 10.1021/jp405383f · Source: PubMed

CITATION

1

READS

115

## 3 AUTHORS:



**Thorsten Koeddermann**

Fraunhofer Institute for Algorithms and Scient...

27 PUBLICATIONS 754 CITATIONS

SEE PROFILE



**Dirk Reith**

Hochschule Bonn-Rhein-Sieg

63 PUBLICATIONS 1,412 CITATIONS

SEE PROFILE



**Axel Arnold**

Universität Stuttgart

56 PUBLICATIONS 1,206 CITATIONS

SEE PROFILE

# Why the Partition Coefficient of Ionic Liquids Is Concentration-Dependent

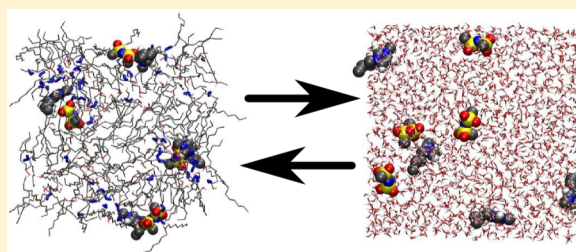
Thorsten Köddermann,<sup>†</sup> Dirk Reith,<sup>§,†</sup> and A. Arnold<sup>\*,†,‡</sup>

<sup>†</sup>Fraunhofer-Institute for Algorithms and Scientific Computing (SCAI), Schloss Birlinghoven, 53754 Sankt Augustin, Germany

<sup>‡</sup>Institute for Computational Physics, Universität Stuttgart, Allmandring 3, 70569 Stuttgart, Germany

<sup>§</sup>Bonn-Rhein-Sieg University of Applied Studies, Grantham-Allee 20, 53757 Sankt Augustin, Germany

**ABSTRACT:** The partition coefficient of a substance measures its solubility in octanol compared with water and is widely used to estimate toxicity. If a substance is hardly soluble in octanol, then it is practically impossible for it to enter (human) cells and therefore is less likely to be toxic. For novel drugs it might be important to penetrate the cell through the membrane or even integrate into it. While for most simple substances the partition coefficient is concentration-independent at low concentrations, this is not true for a few important classes of complex molecules, such as ionic liquids or tensides. We present a simple association–dissociation model for concentration dependence of the partition coefficient of ionic liquids. Atomistic computer simulations serve to parametrize our model by calculating solvation free energies in water and octanol using thermodynamic integration. We demonstrate the validity of the method by reproducing the concentration-independent partition coefficients of small alcohols and the concentration-dependent partition coefficient of a commonly used ionic liquid, 1-butyl-3-methylimidazolium bis-(trifluoromethylsulfonyl)imide  $[C_4MIM][NTf_2]$ . The concentration dependence is accurately predicted in a concentration range of several orders of magnitude.



## INTRODUCTION

For successful drug design or to estimate the toxicity, the activity, or the hydrophobicity of chemicals, a correct understanding of the interactions of a given solute in both aqueous (hydrophilic) and biological (lipophilic) media is important.<sup>1–4</sup> In this regard, the partition coefficient between 1-octanol and water is a key input parameter used to quantify structure–property relationships (QSPRs) of many solute properties.<sup>5</sup> Especially in the pharmaceutical industry, the prediction of drug partitioning, hydrophobicity, and even pharmacokinetic characteristics in biological systems can be quantified by expressions based on the 1-octanol/water partition coefficient  $P_{O/W}$  (commonly reported as  $\log P_{O/W}$ ).<sup>2,3,6</sup> For ionizable species, such as ionic liquids, the partition coefficient is frequently reported as distribution coefficient. This reflects the fact that these species are at least partially ionized in the water phase. If the substance does not fully dissociate, then the distribution coefficient is even pH-dependent.

For most chemical compounds the partition coefficient is concentration-independent for a wide range of (low) concentrations, but for substances like ionic liquids or micelle-forming surfactants there is a significant concentration dependence, which is due to the fact that these substances behave very differently in water and octanol. Recently, this was experimentally shown for the ionic liquid  $[C_4MIM][NTf_2]$  by Lee et al.<sup>7</sup> and Ventura et al.<sup>8</sup> This fact has to be taken into account if one wants to investigate the environmental hazard of

these substances. Both groups explain this behavior by the association and dissociation of ion pairs; however, only Ventura et al. took the macroscopic charge neutrality correctly into account.

Apart from experiments, many different approaches have been developed in an attempt to estimate  $P_{O/W}$ . In the beginning, mostly semiempirical approaches based on the sum of fragment contributions or atom-derived group equivalents were proposed.<sup>1–3,9</sup> Nowadays, fragment additive schemes remain a standard method to estimate solvation free energies and partition coefficients,<sup>10</sup> together with procedures based on QSPR that relate partition coefficients or solvation properties to other molecular properties.<sup>11–13</sup> Although these methods are considerably fast and applicable to whole databases of molecular structures, they require large multiparameter tables, having the disadvantage that whenever new compounds are under study these need to be similar to the ones contained in the training set. This is evidenced by the lack of existing parameters to calculate  $P_{O/W}$  for new chemical groups.<sup>14–16</sup> Thus QSPR methods are based on statistics rather than physics and cannot provide insight into the causes resulting in a certain  $P_{O/W}$ . Simulations based on linear response theory and molecular descriptors to derive empirical relationships for estimating  $P_{O/W}$  have been carried out by Duffy and

Received: May 31, 2013

Revised: August 20, 2013

Published: August 21, 2013

Jorgensen.<sup>17</sup> Finally, approaches based on continuum models have also been investigated.<sup>14,15,18</sup>

Since the 1990s, some molecular simulation studies investigating  $P_{O/W}$  values have been published. Relative water/tetrachloromethane partition coefficients for small alcohols (methanol–ethanol, ethanol–propanol) were calculated utilizing perturbation theory in 1992 by Essex et al.<sup>19</sup> Lennard-Jones as well as Coulombic parameters for the alcohols were altered to investigate their effect on the relative partition coefficient. The TIP3P model<sup>20</sup> was chosen for water. The authors concluded that the results for the methanol/ethanol system do not depend on the used force field, while for the ethanol/propanol system conformation-weighted charges perform much better than single conformation charges.

In 1995, DeBolt et al.<sup>21</sup> computed the relative octanol/water partition coefficient between benzene and phenol and investigated the liquid structure of the solutes in both phases. The authors used molecular dynamics simulation and the free-energy perturbation method. For water, they employed the SPC model,<sup>22</sup> for octanol, a slightly modified version of the OPLS force field.<sup>23</sup> Their results deviate from the experimental data by 0.09 log  $P_{O/W}$  units. Similar work was performed by Best et al.<sup>14</sup> The authors took the TIP3P water model as well as the all-atom OPLS force field for octanol and the solutes to calculate relative partition coefficients for seven molecule pairs utilizing free-energy perturbation. They got results in the same error range as DeBolt et al.

The expanded ensemble (EE) method was used by Lyubartsev et al.<sup>24</sup> to simulate octanol/water partition coefficients for a set of drug-related compounds. The SPC model was used for the water, and CHARMM and OPLS force fields were used for the octanol and the solute. The authors compared their simulated results with three commonly used  $P_{O/W}$  prediction programs (logP calculator from Advanced Chemistry Developments, HyperChem from HyperCube, and the prologP module of Pallas from CompuDrug International). The conclusion drawn in this study was that the accuracy of the MD simulation is comparable to that of the tested programs. For molecules, however, that are not a part of the training set of the prediction software, MD simulation may give better results.

Configurational-bias Monte Carlo simulations in the Gibbs ensemble using the TIP4P and OPLS force fields were performed by Chen et al.<sup>25</sup> to study the Gibbs free energy of transfer for *n*-alkanes and primary alcohols between water, neat or water-saturated 1-octanol, and helium vapor phases. The results deviate very much from experimental data. Furthermore, the authors showed that the OPLS/TIP4P system is not able to simulate the correct concentration of water in octanol and concluded that accurate simulations require a next generation of force fields explicitly treating polarization effects.

To understand the *in vivo* pharmacokinetic profile of new drug candidates, de Oliveira et al.<sup>26</sup> calculated the relative octanol/water partition coefficients of benzamine derivatives by using MD simulation in conjunction with the finite difference thermodynamic integration algorithm (FDTI). The all-atom CVFF force field<sup>27</sup> was used. The authors measured one partition coefficient themselves and compared their result with the simulated coefficient. Experimental and simulation results agree very well with each other; however, the error bars for both are rather large.

In 2009, Garrido et al.<sup>28</sup> investigated the octanol/water partition coefficients of *n*-alkanes (chain length 1 to 8). The authors tested several force-field combinations (TraPPE,<sup>29</sup>

Gromos,<sup>30</sup> OPLS-AA/TraPPE, Gromos/OPLS-AA/TraPPE) using the MSPC/E force field for water.<sup>31</sup> They concluded that the most accurate  $P_{O/W}$  predictions are afforded by the Gromos force field for *n*-alkanes in the water phase and the combination of the OPLS-AA force field for *n*-alkanes with the TraPPE force field for octanol in the organic phase, reaching absolute deviations to experimental data of 0.1 log  $P_{O/W}$  units. We believe, however, that such a combinatoric approach may not be quantitatively accurate. That is why we chose to individually parametrize our model, that is, the force field. The second best results were obtained by the TraPPE force field with deviations of 0.3 log  $P_{O/W}$  units from experiment. Garrido et al. expanded their study and investigated the total solvation free enthalpy in water for polar molecules like alcohols, ibuprofen, or benzoic acid.<sup>32</sup> For monofunctional molecules, all investigated force fields give reasonable results. For multifunctional molecules, however, the tested force fields show limitations. This leads the authors to the conclusion that reparameterization of the partial atomic charges of multifunctional molecules is necessary.

All of the above-mentioned simulation studies estimate the partition coefficient only in the infinite dilution limit and therefore cannot be used for substances with a concentration-dependent  $P_{O/W}$ . We present an approach to quantify the concentration-dependent octanol/water partition coefficient using a combination of theoretical considerations and computer simulations to estimate solvation free energies. It extends the approach of Garrido et al.<sup>28</sup> based on thermodynamic integration, while the necessary theoretical model for the IL partition coefficient is based on the model of Ventura et al.<sup>8</sup>

We test our approach on small alcohol molecules and demonstrate that our approach allows us to obtain better approximations for the partition coefficient than heuristic approaches.<sup>33</sup> More importantly we show that quantitative simulation of concentration-dependent partition coefficients of an ionic liquid is also possible, utilizing the TIP4P-2005<sup>34</sup> and the TraPPE force field<sup>35</sup> as well as a self-parametrized united atom force field for the ionic liquid [C<sub>4</sub>mim][NTf<sub>2</sub>].<sup>36</sup>

## METHOD

Experimentally, the partition coefficient is determined by mixing equal amounts of water and water-saturated octanol and a small amount of the solute in question. After letting the system rest, the concentration of the solute in both phases is measured to determine the concentration ratio

$$P_{O/W} = \frac{c_o}{c_w} = \frac{N_o}{N_w} \quad (1)$$

Here  $c_w$  and  $c_o$  denote the concentrations of solute molecules in the water and water-saturated octanol phase, respectively, and  $N_o$  and  $N_w$  are the corresponding numbers of molecules. The equivalence is due the fact that both phases have equal volume  $V$ . Usually, the partition coefficient is assumed to be concentration-independent so that the “small amount” of the solute does not need to be specified more quantitatively, but because we are interested in the concentration-dependent partition coefficient, we assume in the following a finite concentration  $c_i$  of the solute in the initial mixed phase.

Performing the mixing process directly in computer simulations is impossible because any feasible system size would be so small that surface effects at the water–octanol interface dominate. However, in computer simulations we can

consider two independent compartments that represent the two phases. In equilibrium, the numbers  $N_w$  and  $N_o$  of solute molecules in the water and water-saturated octanol phase, respectively, are determined by the condition of equal chemical potential:

$$\ln N_w + \beta \mu_{\text{ex},w}(N_w/V) = \ln N_o + \beta \mu_{\text{ex},o}(N_o/V) \quad (2)$$

where  $\mu_{\text{ex}}(\rho)$  denotes the excess chemical potential at solute number density  $\rho$ ,  $\beta = 1/k_B T$ , and  $V$  denotes the equal volume of both compartments. Therefore

$$\ln P_{O/W} = \ln \frac{N_o}{N_w} = \beta [\mu_{\text{ex},w}(N_w/V) - \mu_{\text{ex},o}(N_o/V)] \quad (3)$$

Note that literature values for  $\log P_{O/W}$  are decimal logarithms, that is,  $\log P_{O/W} = \ln P_{O/W} / \ln 10$ .

As described, only a small amount of solute is added, and if the solute dissolves reasonably well in both phases, the solute molecules barely interact, and  $\mu_{\text{ex}}$  is independent of the concentration. In this case, one can measure in the infinite dilution limit, that is, with a single solute molecule in the host phase.<sup>28,32,35</sup> However, if the solute, for example, tends to agglomerate or dissociate in one of the phases, the excess chemical potentials can be concentration-dependent. Because of the fixed total number  $N = N_w + N_o$  of added molecules, this leads to the equation

$$\ln P_{O/W} = \ln \frac{N - N_w}{N_w} = \beta [\mu_{\text{ex},w}(N_w/V) - \mu_{\text{ex},o}((N - N_w)/V)] \quad (4)$$

which has to be solved numerically once the functions  $\mu_{\text{ex},w}(c)$  and  $\mu_{\text{ex},o}(c)$  are determined. In terms of concentrations, this reads

$$\ln P_{O/W} = \ln \frac{2c_i - c_w}{c_w} = \beta [\mu_{\text{ex},w}(c_w) - \mu_{\text{ex},o}(2c_i - c_w)] \quad (5)$$

where  $c_i = N/2V$  is the initial concentration of solute in the total mixture and  $c_w = N_w/V$  is the concentration of solute in the water phase. Note that computer simulations only allow us to measure  $\mu_{\text{ex},w}(c)$  and  $\mu_{\text{ex},o}(c)$  at specific concentrations. These cannot be turned into continuous functions by classical methods like interpolation because atomistic computer simulation results are usually too noisy for this. However, one can often deduct a simple model for  $\mu_{\text{ex}}(c)$ , which then is easily parametrized by the simulation data.

For the special case of ionic liquids, we follow the model of ref 8, which explains the concentration dependence by the different degree of dissociation in the water and octanol phases. Our derivation differs in that we base our work on chemical potentials, which are easy to measure in computer simulations. Our simulation data will justify this model later.

We consider first one of the two phases. The chemical potential of an ion pair is

$$\mu_p = k_B T \ln N_p + \mu_{\text{ex},p} \quad (6)$$

and that of a free cation or anion is

$$\mu_{+/-} = k_B T \ln N_{+/-} + \mu_{\text{ex},+/-} \quad (7)$$

Note that to exploit the fact that the water and octanol phases have equal volume we use particle numbers rather than

concentrations so that a constant  $\ln V$  is adsorbed into the excess chemical potentials  $\mu_{\text{ex}}$ .

We assume that  $\mu_{\text{ex},p}$  and  $\mu_{\text{ex},\pm}$  are constants independent of the number of particles. This is equivalent to neglecting interactions between both associated and dissociated ion pairs as well as dissociated anions and cations. This assumption is justified due to the low concentrations at which the partition coefficient is usually measured. Furthermore, we assume that the ionic liquid is not strong enough to change the pH of the water phase significantly. Then, there can be dissociated ion pairs but never any macroscopic charge excess because the latter would have to be balanced by a corresponding partition of  $\text{HO}^-/\text{H}_3\text{O}^+$  to maintain macroscopic electroneutrality. Therefore,  $N_+ = N_- =: N_d$ , where  $N_d$  denotes the number of dissociated ion pairs. This simplifies eq 7 to

$$\mu_d = 2k_B T \ln N_d + \mu_{\text{ex},d} \quad (8)$$

where  $\mu_{\text{ex},d} := \mu_{\text{ex},+} + \mu_{\text{ex},-}$ . Note that  $\mu_{\text{ex},d}$  is only a constant and not the excess chemical potential of a dissociated ion pair, which is  $k_B T \ln N_d + \mu_{\text{ex},d}$  and thus not constant. Because dissociated and bound ion pairs can freely exchange through association and dissociation, the chemical potentials given by eqs 6 and 8 must be equal in equilibrium, which leads to the relation

$$\frac{N_p}{N_d^2} = e^{\beta(\mu_{\text{ex},d} - \mu_{\text{ex},p})} =: K \quad (9)$$

which is the law of mass action. Note that the constant  $K$  becomes proportional to the volume if concentrations rather than particle numbers are considered.

For a total number of ions  $N$ , this means that

$$N_p = N + \frac{1}{2K} - \sqrt{\frac{N}{K} + \frac{1}{4K^2}} \quad (10)$$

and the chemical potential of an ion pair, bound or dissociated, is

$$\begin{aligned} \mu = \mu_d = \mu_p &= k_B T \ln \left( N + \frac{1}{2K} - \sqrt{\frac{N}{K} + \frac{1}{4K^2}} \right) + \mu_{\text{ex},p} \\ &= k_B T \ln N + \mu_{\text{ex}} \end{aligned} \quad (11)$$

where

$$\mu_{\text{ex}} = k_B T \ln \left( 1 + \frac{1}{2KN} - \sqrt{\frac{1}{KN} + \frac{1}{4K^2 N^2}} \right) + \mu_{\text{ex},p} \quad (12)$$

which can be plugged into (eq 4). The expression in terms of concentrations can be obtained by simply replacing  $N$  by  $c$ . If  $K$  is very large, that is, practically all ion pairs are associated, then eq 11 reduces to  $\mu_{\text{ex}} \approx \mu_{\text{ex},p}$ , as expected. In the limit of small  $K$ , that is, full dissociation, this reduces to  $\mu_{\text{ex}} \approx k_B T \ln N + \mu_{\text{ex},d}$ , accounting for the larger entropy of dissociated ion pairs. These considerations can be extended to other substances forming larger aggregates by considering the corresponding entropy loss. By analogy to the bound and unbound ion pairs, one considers an aggregate of average size and an equal amount of unbound solute molecules. Of course, for this simplification, the size distribution of aggregates should be rather narrow, as is the case for example for micelles. In this case, one considers the balance between an aggregate and an equal amount of free solute molecules. The free solute molecules have a chemical



Table 1. Molecule Composition of the Systems Simulated in This Work

system	water phase	octanol phase
alcohols	554 water, 1 alcohol	128 water, 512 octanol, 1 alcohol
IL 6 mmol/L	9400 water, 1 ion pair	264 water, 1056 octanol, 1 ion pair
IL 10 mmol/L	25880 water, 4 ion pairs	724 water, 2898 octanol, 4 ion pairs
IL 22 mmol/L	9994 water, 4 ion pairs	278 water, 1113 octanol, 4 ion pairs
IL 36 mmol/L	6104 water, 4 ion pairs	170 water, 680 octanol, 4 ion pairs
IL 100 mmol/L	2216 water, 4 ion pairs	62 water, 248 octanol, 4 ion pairs

potential of  $N_m$  ( $k_B T \ln N_d + \mu_{\text{ex,d}}$ ), where  $N_m$  denotes the size of a typical aggregate and  $\mu_{\text{ex,d}}$  is the excess chemical potential of a single solute molecule, which can be determined by thermodynamic integration as well as the chemical potential of the aggregate.

## SIMULATION DETAILS

Classical molecular dynamics simulations combined with thermodynamic integration were carried out to calculate the octanol/water partition coefficient  $P_{O/W}$  of alcohols with chain length  $n = 1, 2, 4$  and, more importantly, of the ionic liquid [C<sub>4</sub>MIM][NTf<sub>2</sub>] at different concentrations. The simulations took place in the isobaric–isothermal (NPT) ensemble at 298 K and 1 bar.

The molecule composition of the systems simulated in this work is shown in Table 1. Note that the alcohol simulations as well as the IL simulations at 6 mmol/L contain only one solute molecule to avoid simulating excessive amounts of solvent. The 1/4 water/octanol ratio, which corresponds to a saturated solution, was taken from DeBolt et al.<sup>21</sup>

As investigated in ref 28, the TrAPPE force field performs well in reproducing partition coefficients. Thus the TrAPPE model<sup>35</sup> together with the TIP4P-2005 water model<sup>34</sup> were used in this study for the alcohols. However, a reparameterized force field was created for the ionic liquid.<sup>36</sup> It could be designed quickly and robustly by way of utilizing our semiautomated optimization algorithms.<sup>37,38</sup> All force fields are represented by a sum of pairwise additive inter- and intra-atomic Lennard-Jones and Coulombic potentials as well as angle and torsion potentials:

$$U = \sum_{ijk}^{\text{angles}} \frac{k_a}{2} (\theta_{ijk} - \theta_0) + \sum_{ijkl}^{\text{dihedrals}} \sum_{m=1}^n k_d (1 + \cos(m\psi - \psi_0)) + \sum_{i=1}^{N-1} \sum_{j>1}^N [U^{\text{LJ}}(r_{ij}) + U^{\text{Coul}}(r_{ij})] \quad (13)$$

with

$$U^{\text{LJ}}(r_{ij}) = 4\epsilon_{ij} \left[ \left( \frac{\sigma_{ij}}{r_{ij}} \right)^{12} - \left( \frac{\sigma_{ij}}{r_{ij}} \right)^6 \right]$$

and

$$U^{\text{Coul}}(r_{ij}) = \frac{q_i q_j}{4\pi\epsilon_0 r_{ij}}$$

The simulations were carried out using the Gromacs-4.0.5 package.<sup>39</sup> Electrostatic interactions were computed using the smooth particle mesh Ewald summation<sup>40</sup> with a real space cutoff of 1.2 nm and a mesh spacing of 0.12 nm and fourth-order interpolations. The 1–4 interactions of all molecules are

switched off. The OPLS combining rules are applied. All bond lengths were fixed. A time step of 2 fs was used, temperature control was achieved using a Nosé–Hoover thermostat, and a pressure control was achieved using a Rahman–Parrinello barostat with coupling times  $\tau_t = 0.5$  ps and  $\tau_p = 2.0$  ps, respectively. In the case of the alcohol simulations, a 500 ps equilibration run followed by a 5.5 ns production run was performed. The ionic liquid system was equilibrated for 500 ps, and the production run took 7.5 ns.

For the thermodynamic integration, we gradually switched on all interactions between the inserted solute molecule. A switching parameter  $\lambda$  was used to scale the charges and the Lennard-Jones parameters using the softening of the singularity as described in ref 39. The parameters  $sc\_alpha$  and  $sc\_power$  were set to 2.0 and 2.0, respectively.  $\lambda$  was sampled between 0 (the solute molecule behaves like an ideal gas particle) and 1 (it interacts regularly), within 42 steps. Note that by this procedure, we obtain the excess chemical potential  $\mu_{\text{ex}}$  which we can directly insert into eq 3. The full chemical potential is  $k_B T \ln N_d + \mu_{\text{ex}}$  where  $N$  is the number of solute molecules.

In the case of the ionic liquid, we insert simultaneously cation and anion, that is, a complete ion pair, as “molecule” to ensure electrostatic neutrality. The interactions between cation and anion were switched on gradually like all interactions so that for  $\lambda = 0$  the ions effectively behave like two ideal gas particles, which explore the phase space independently. Consequently, what we measure in the ionic liquid simulations is  $\tilde{\mu}_{\text{ex}} = \mu - 2k_B T \ln N$ . To be consistent with method description, we report  $\mu_{\text{ex}} = k_B T \ln N + \tilde{\mu}_{\text{ex}}$  as the excess chemical potential of the ion pair in the following.

## RESULTS AND DISCUSSION

**Small Alcohols.** To demonstrate the basic principles of our method, we apply it to small alcohols, where  $P_{O/W}$  is concentration-independent. In this case, our method is identical to the approach by Garrido et al.<sup>28</sup> The free energies of solvation are obtained by thermodynamic integration, where the interactions of one of the solute molecules with the solvent, that is, water or water-saturated octanol, are parametrized by a parameter  $\lambda$ . For  $\lambda = 0$ , the solute molecule does not interact with the solvent, while at  $\lambda = 1$ , it is fully interacting like any another molecule in the simulation. Figures 1 and 2 verify that the derivative of the free energy,  $G'(\lambda)$ , is within reasonable bounds; in particular, there is no indication that we cross a phase boundary. The values at small  $\lambda$  reflect internal differences between the different alcohols considered. The dip in the water phase marks the point where the water molecules rearrange to accommodate the solute molecule. For the larger butanol molecule, more rearrangement is necessary, leading to a deeper minimum.

By integrating  $G'(\lambda)$ , one obtains the solvation free energy. As one can see, the differences in  $G'(\lambda)$  are small between the different alcohols compared with the maximal and minimal

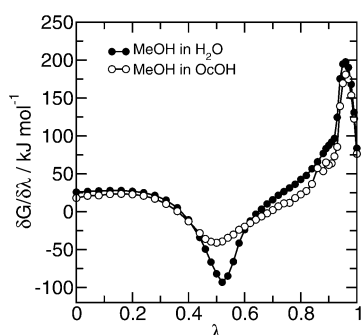


**Figure 1.** Derivative  $G'(\lambda)$  of the free energy as a function of the interaction scaling parameter  $\lambda$  for methanol in water and saturated octanol. At  $\lambda = 0$ , the alcohol is not interacting with the rest of the system; at  $\lambda = 1$ , a regular MD with unscaled interactions is performed. The main differences between water and octanol are around  $\lambda = 0.5$ , where the solute molecule locks into the different solvent structures.

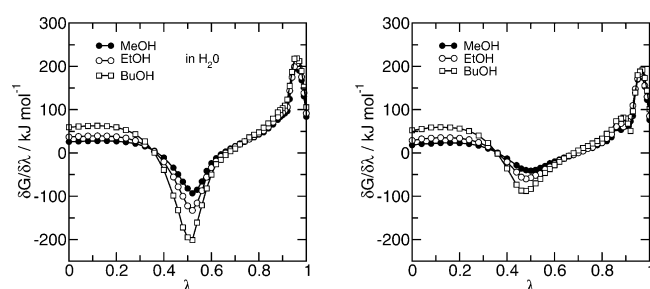


**Figure 2.** Derivative  $G'(\lambda)$  of the free energy as a function of the interaction scaling parameter  $\lambda$  for different small alcohols in water (left) and saturated octanol (right). Differences at  $\lambda = 0$  are solely due to the internal structure of the solute, the main difference, however, is again due to the different arrangement in the solvent structure.

values of  $G'(\lambda)$ . Therefore, the simulations need to be rather well equilibrated. We want to stress that the simulations for each  $\lambda$  were performed independently, so that the smoothness of the curves in Figure 1 and Figure 2 can serve to demonstrate the reliability of our simulation data.

However, more importantly, our results also reproduce known experimental results, as is shown in Table 2, which shows the free energies of solvation of the investigated alcohols in water and octanol. The  $\log P_{O/W}$  values are obtained from (eq 3), assuming concentration-independence of the solvation free energies. These values are compared with experimental values;<sup>25,41</sup> not only do the simulations reproduce the overall trend correctly but also the absolute deviations between experiment and simulation are satisfactorily small. The approach using free energies of solvation also compares favorably to heuristic approaches, as they are commonly used to predict  $\log P_{O/W}$  values. Figure 3 demonstrates this by comparison with the widely used X-SCORE software.<sup>33</sup>

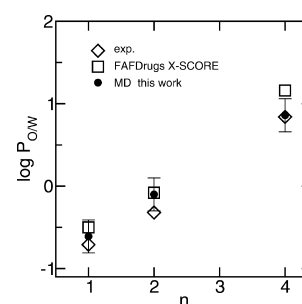


**Figure 3.**  $\log P_{O/W}$  values as a function of alkyl chain length  $n$  compared with experimental data as well as to data generated with the program X-SCORE.

**Ionic Liquid: [C<sub>4</sub>mim][NTf<sub>2</sub>].** As an example of a substance that has a concentration-dependent octanol/water partition coefficient, we consider the ionic liquid [C<sub>4</sub>mim][NTf<sub>2</sub>]. For this ionic liquid, experimental data on the concentration dependence are available.<sup>7</sup>

We use eq 5 to calculate the concentration dependent  $P_{O/W}$ . Numerically solving this equation requires an analytically available estimate for the chemical potentials, which we obtain from our model of associated or dissociated ion pairs. To determine the required chemical potentials of ion pairs in the water and octanol phases, we have measured the concentration-dependent free energies of solvation using thermodynamic integration. As described, the ion pair, that was inserted during the integration, was free at  $\lambda = 0$  but interacting completely normal at  $\lambda = 1$ . In particular, the ion pairs were free to associate or dissociate, and during the 8 ns long simulations we typically observed association and dissociation events.

Figure 4 exemplarily shows the free-energy derivative  $G'(\lambda)$  at different concentrations. Again, points for different  $\lambda$  have

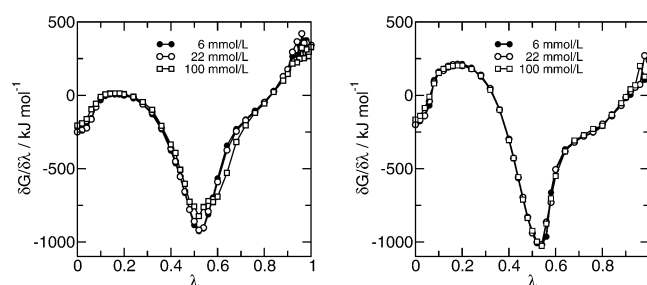


**Figure 4.** Derivative of the free energy  $G'(\lambda)$  as a function of the interaction scaling parameter  $\lambda$  for [C<sub>4</sub>mim][NTf<sub>2</sub>] in water (left) and saturated octanol (right) at different concentrations. Note that the differences between the concentrations are very small, however, systematic. Therefore, they still lead to considerable differences when integrated.

**Table 2.** Comparison of  $\log P_{O/W}$  Values for Different Alcohols<sup>a</sup>

solute	$G_O$	$G_W$	$\Delta G_{\text{sim}}$	$\Delta G_{\text{exp}}$	$\log P_{\text{sim}}$	$\log P_{\text{exp}}$	deviation
methanol	−17.36	−20.84	3.48	4.05	−0.61 ± 0.2	0.71	0.10
ethanol	−18.93	−19.49	0.56	1.80	−0.10 ± 0.2	−0.32	0.22
butanol	−23.66	−18.73	−4.93	−4.78	0.86 ± 0.2	0.84	0.02

<sup>a</sup>Given are the simulated solvation free energies  $G_O$  in octanol,  $G_W$  in water, and their difference  $\Delta G_{\text{sim}} = G_O - G_W$  as obtained from our simulations. From this, we determined the partition coefficient  $\log P_{\text{sim}} = \beta \Delta G_{\text{sim}}$ . For comparison, we include experimental results, namely, the measured free-energy difference  $\Delta G_{\text{exp}}$  as well as the resulting experimental  $\log P_{\text{exp}}$  values.<sup>3</sup> All energies are given in kJ/mol.

been obtained by independently equilibrated simulations; therefore, the Figure shows that the data are well-converged and suitable to calculate the free energies of solvation. However, the Figure also shows that the differences between different concentrations are significantly smaller than the differences between the small alcohols. Therefore, we were still able to extract free energies of solvation but with considerable relative errors. This is despite the fact that we have used considerably more computational power for the ionic liquid than for the alcohols.

Figure 5 shows the obtained excess chemical potential as a function of the IL concentration in the water and octanol

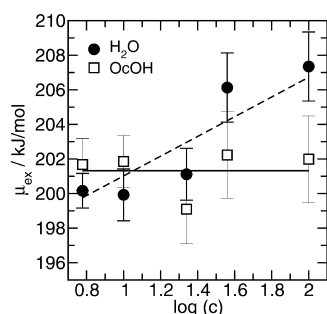


**Figure 5.** Free energies of solvation  $\mu_{\text{ex}}$  in water (full circles) and octanol (open squares) as a function of the IL concentration  $c$  in the respective phase. The data spread is considerable, but the trend fits to the model (eq 11). In the water phase, the data are best described as fully dissociated ion pairs with an excess chemical potential of  $\mu_{\text{ex}} = 195.3 \text{ kJ/mol} + k_B T \ln c$ . In octanol, the data can be described by a constant  $201.3 \text{ kJ/mol}$ , meaning that ions are mostly associated.

phases. The spread of the data is only about  $2 \text{ kJ/mol}$ . However, this is the same magnitude as the differences in chemical potential between the different concentrations. Note also that the simulation setups for the lowest and next higher concentration are quite different because we use only a single ion pair at the lowest concentration but four ion pairs in a larger simulation box for the next higher concentration. The results nevertheless are very similar up to the apparent error, showing that the data are reliable.

To apply our association/dissociation model for the ion pairs, we fit eq 12 to our measured chemical excess potentials. Equation 12 has in each phase two free parameters, corresponding to very low and high concentrations. However, the fitting is facilitated by the fact that the chemical excess potential in octanol seems to be constant within the accuracy of the data, as Figure 5 shows. This is not surprising and reflects the fact that the ionic liquid is mostly associated, similar to the grouping of the polar head groups. We have therefore chosen  $K = \infty$  in octanol. In water, the chemical potential grows with the logarithm of the concentration, a clear indication that the ions are completely dissociated. Consequently, we have chosen  $K = 0$ . Note that in both water and octanol, the only fit parameter is the chemical potential offset, while the slope is fully determined by our assumption on  $K$ , which seems to agree well with our data.

Figure 6 shows the integrated radial density  $I_{\text{cat-an}}(r)$  of cations around anions (or vice versa) in water and octanol at a concentration of  $36 \text{ mmol/L}$ .  $I_{\text{cat-an}}(r)$  gives the average number of cations in a sphere of radius  $r$  around any anion. In octanol, the function reaches a count of one counterion within  $1 \text{ nm}$ , that is, in close contact. In conjunction with the strong

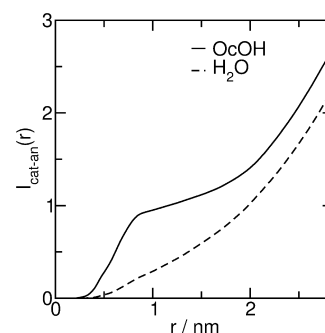


**Figure 6.** Integrated radial density  $I_{\text{cat-an}}$  of cations around anions in the octanol and water phases. Only in octanol, a distinct shoulder at a distance of  $1 \text{ nm}$  shows the presence of ion pairs. In water, the ions are mostly dissociated, since  $I_{\text{cat-an}}$  is mostly featureless.

shoulder, this is a clear indication that in octanol the ions are practically always forming ion pairs. In water, the chance of finding a counterion within  $1 \text{ nm}$  is  $<30\%$ , which is simply due to the average concentration of ions. This can be seen from the fact that the integrated density has no distinct features. This confirms that there is a strong association of cations and anions in octanol, while they are only weakly interacting in water.

Using the excess chemical potentials estimates  $\mu_{\text{ex,w}} = 195.3 \text{ kJ/mol} + k_B T \ln c_w$  in water, where  $c_w$  denotes the concentration of ionic liquid in water and  $\mu_{\text{ex,w}} = 201.3 \text{ kJ/mol}$  in octanol, the resulting estimated  $\log P_{\text{O/W}}$  as a function of the concentration  $2c_i$  in the initial, mixed phase is shown in Figure 7. Our model reproduces the experimental concen-

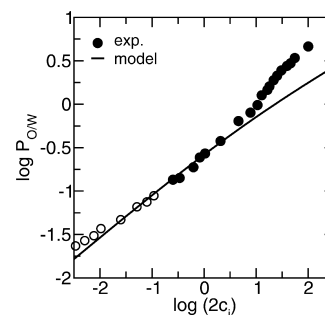


**Figure 7.** Calculated  $\log P_{\text{O/W}}$  values as a function of initial concentration of  $[\text{C}_4\text{MIM}][\text{NTf}_2]$  compared with experimental data from ref 7. Open symbols refer to a different experimental technique<sup>7</sup> due to difficulties studying low concentrations.

tration-dependent  $\log P_{\text{O/W}}$  over a large range. Please note that the initial concentration as reported in this Figure is not directly related to the concentrations, for which the chemical potentials were measured, because for  $P_{\text{O/W}} \neq 1$  the concentrations in the water or octanol phases very strongly differ from the initial concentrations. For example, for an initial concentration of  $100 \text{ mmol/L}$ , the experimental  $\log P_{\text{O/W}}$  is approximately  $0.7$ , and the resulting concentrations in the water and octanol phases are  $33$  and  $166 \text{ mmol/L}$ , which is outside the considered range of chemical potentials.

Deviations occur mostly at high initial concentrations with positive  $\log P_{\text{O/W}}$ , that is, with high concentrations of ion pairs in the octanol phase. This can be expected, as the ionic liquid might form more complex aggregates than just ion pairs in the water pockets of the octanol phase. However, the currently achievable computational accuracy is not sufficient to

investigate such details. Nevertheless, our model combined with the input data from the simulations is clearly well-suited to predict the concentration-dependent  $\log P_{O/W}$ .

## CONCLUSIONS

Using thermodynamic integration, one can obtain the free energies of solvation in water and water-saturated octanol, which can be used to calculate  $P_{O/W}$ , as we have shown. This allows us to reliably determine the octanol/water partition coefficient *in silico* without the need to refer to reference experimental data. Of course, this requires force fields that accurately describe the solvation behavior of the substance in question. Our computer simulations of small alcohols demonstrate the feasibility of this method, even using standard force fields. Unlike heuristic approaches estimating the  $P_{O/W}$  based on databases of chemical compounds, our method is systematic and therefore can be applied to substances, which cannot be decomposed into simple compounds easily. Also, the inclusion of new chemical functional groups is not limited by the availability of experimental data for training.

As we have shown, the concentration-dependent  $P_{O/W}$  can also be determined from numerically solving an equation for the concentration-dependent free energies of solvation. However, this requires an analytic model for concentration dependence. For the case of ionic liquids, we use the model of Ventura et al.,<sup>8</sup> which explains the concentration dependence by partial dissociation of ion pairs. An application to other substances with concentration-dependent partition coefficients, such as tensides, is possible following a similar modeling.

The association/dissociation model for the ion pairs was a posteriori justified not only by the available experimental data but also by our simulations. For the ionic liquid [C<sub>4</sub>mim]-[NTf<sub>2</sub>], we were able to reproduce the experimental concentration dependence of the partition coefficient for three orders of magnitude so that we are fairly confident that our simulations match the experimental conditions. Our results show that the ionic liquid is indeed mostly dissociated in water but mostly associated into ion pairs in the octanol phase. The concentration dependence of the partition coefficient is therefore in this case solely due to entropic reasons, namely, dissociation of ion pairs.

## AUTHOR INFORMATION

### Corresponding Author

\*E-mail: arnolda@icp.uni-stuttgart.de.

### Notes

The authors declare no competing financial interest.

## ACKNOWLEDGMENTS

A.A. thanks P. Košov, M. Sega, and S. Kesselheim for very fruitful discussions on the calculation of the chemical potentials. We thank Stefan Grundei and the Klüber Lubrication KG for continued interest and financial support.

## REFERENCES

- (1) Leo, A.; Hansch, C.; Elkins, D. *Chem. Rev.* **1971**, *71*, 525–616.
- (2) Hansch, C.; Leo, A.; Hoekman, D. *Exploring QSAR: Hydrophobic, Electronic and Steric Constants*; American Chemical Society: Washington, DC, 1995.
- (3) (a) Sangster, J. *Octanol-Water Partition Coefficients: Fundamentals and Physical Chemistry*; John Wiley & Sons: Chichester, U.K., 1997. (b) Dallas, A. J.; Carr, P. E. *J. Chem. Soc., Perkin. Trans.* **1992**, *2*, 2155–2161.
- (c) Cabani, S.; Gianni, P.; Mollica, V.; Lepori, L. *J. Solution Chem.* **1981**, *10*, 563–595.
- (4) Perlovich, G. L.; Kurkov, S. V.; Kinchin, A. N.; Bauer-Brandl, A. *AAPS PharmSciTech* **2004**, *6*, 1–9.
- (5) Hansch, C.; Leo, A.; Hoekman, D. *Exploring QSAR: Fundamentals and Applications in Chemistry and Biology*; American Chemical Society: Washington, DC, 1995.
- (6) Betageri, G. V.; Rogers, J. A. *Pharm. Res.* **1989**, *6*, 399–403.
- (7) Lee, S. H.; Lee, S. B. *J. Chem. Technol. Biotechnol.* **2009**, *84*, 202.
- (8) Ventura, S. P.; Gardas, R. L.; Goncalves, F.; Coutinho, J. A. *J. Chem. Technol. Biotechnol.* **2011**, *86*, 957.
- (9) Leo, A. *J. Chem. Rev.* **1993**, *93*, 1281–1306.
- (10) Viswanadhan, V. N.; Ghose, A. K.; Singh, U. C.; Wendoloski, J. *J. Chem. Inf. Comput. Sci.* **1999**, *39*, 405–412.
- (11) Bodor, N.; Buchwald, P. *J. Phys. Chem. B* **1997**, *101*, 3404–3412.
- (12) Kamlet, M. J.; Doherty, R. M.; Abraham, M. H.; Marcus, Y.; Taft, R. W. *J. Phys. Chem.* **1988**, *92*, 5244–5255.
- (13) Karelson, M. *Molecular Descriptors in QSAR/QSPR*; Wiley Interscience: New York, 2000.
- (14) Best, S. A.; Merz, K. M.; Reynolds, C. H. *J. Phys. Chem. B* **1999**, *103*, 714–726.
- (15) Curutchet, C.; Orozco, M.; Luque, F. J. *J. Comput. Chem.* **2001**, *22*, 1180–1193.
- (16) Westergren, J.; Lindfors, L.; Hoglund, T.; Luder, K.; Nordholm, S.; Kjellander, R. *J. Phys. Chem. B* **2007**, *111*, 1872–1882.
- (17) Duffy, E. M.; Jorgensen, W. L. *J. Am. Chem. Soc.* **2000**, *122*, 2878–2888.
- (18) Orozco, M.; Luque, F. J. *Chem. Rev.* **2000**, *100*, 4187–4225.
- (19) Essex, J. W.; Reynolds, C. A.; Richards, W. G. *J. Am. Chem. Soc.* **1992**, *114*, 3634–3639.
- (20) Jorgensen, W. L.; Chandrasekhar, J.; Madura, J. D.; Impey, R. W.; Klein, M. L. *J. Chem. Phys.* **1983**, *79*, 926–935.
- (21) DeBolt, S. E.; Kollman, A. *J. Am. Chem. Soc.* **1995**, *117*, 5316–5340.
- (22) Toukan, K.; Rahman, A. *Phys. Rev. B* **1985**, *31*, 2643–2648.
- (23) Jorgensen, W. L.; Maxwell, D. S.; Tirado-Rives, J. *J. Am. Chem. Soc.* **1996**, *118*, 11225–11236.
- (24) Lyubartsev, A. P.; Jacobsson, S. P.; Sundholm, G.; Laaksonen, A. *J. Phys. Chem. B* **2001**, *105*, 7775–7782.
- (25) Chen, B.; Siepmann, J. I. *J. Am. Chem. Soc.* **2000**, *122*, 6464–6467.
- (26) De Oliveira, C. A. F.; Guimaraes, C. R. W.; De Mello, H.; Echevarria, A.; De Alencastro, R. B. *Int. J. Quantum Chem.* **2005**, *102*, 542–553.
- (27) Biosym Technologies, 9685 Scranton Road, San Diego, CA 92121-2777.
- (28) Garrido, N. M.; Queimada, A. J.; Jorge, M.; Macedo, E. A.; Economou, I. G. *J. Chem. Theory Comput.* **2009**, *5*, 2436–2446.
- (29) Chen, B.; Potoff, J. J.; Siepmann, J. I. *J. Phys. Chem.* **2001**, *105*, 3093.
- (30) van Gunsteren, W. F. *GROMOS. Groningen Molecular Simulation Program Package*; University of Groningen: Groningen, The Netherlands, 1987.
- (31) Boulougouris, G. C.; Economou, I. G.; Theodorou, D. N. *J. Phys. Chem. B* **1998**, *102*, 1029.
- (32) Garrido, N. M.; Jorge, M.; Queimada, A. J.; Economou, I. G.; Macedo, E. A. *Fluid Phase Equilib.* **2010**, *296*, 110–115.
- (33) X-Score website. <http://sw16.im.med.umich.edu/software/xtool>.
- (34) Abascal, J. L. F.; Vega, C. *J. Chem. Phys.* **2005**, *123*, 234505.
- (35) Chen, B.; Potoff, J. J.; Siepmann, J. I. *J. Phys. Chem. B* **2001**, *105*, 3093–3104.
- (36) Köddermann, T.; Reith, D.; Ludwig, R. *ChemPhysChem* **2013**, DOI: 10.1002/cphc.201300486.
- (37) (a) Hülsman, M.; Köddermann, T.; Vrabec, J.; Reith, D. *Comput. Phys. Commun.* **2010**, *181*, 499. (b) Hülsman, M.; Müller, T. J.; Köddermann, T.; Reith, D. *Mol. Sim.* **2010**, *36*, 1182–92.



- (38) (a) Reith, D.; Kirschner, K. N. *Comput. Phys. Commun.* **2011**, *182*, 2184. (b) Krämer-Fuhrmann, O.; Neisius, J.; Gehlen, N.; Reith, D.; Kirschner, K. N. *J. Chem. Inf. Model.* **2013**, *53*, 802–808.
- (39) van der Spoel, D.; Lindahl, E.; Hess, B.; Groenhof, G.; Mark, A. E.; Berendsen, H. J. C. *J. Comput. Chem.* **2005**, *26*, 1701–1718.
- (40) Darden, T.; Perera, L.; Li, L.; Pedersen, L. *Structure* **1999**, *7*, 55–60.
- (41) RPBS list of log POW values. <http://bioserv.rpbs.jussieu.fr/Help/LogP.html> (accessed July 29, 2011).